

## Supplemental Information

Impact of building block structure on ion transport in cyclopropenium-based polymerized ionic liquids

Benjamin A. Paren<sup>1</sup>, Ramya Raghunathan<sup>2</sup>, Jessica L. Freyer<sup>2</sup>, Isaac Knudson<sup>2</sup>, Luis M. Campos\*<sup>2</sup>, Karen I. Winey\*<sup>1</sup>

<sup>1</sup>University of Pennsylvania, Department of Materials Science & Engineering, Philadelphia, Pennsylvania 19104, United States

<sup>2</sup>Columbia University, Department of Chemistry, New York, New York 10027, United States

\*corresponding authors, e-mail: winey@seas.upenn.edu and lcampos@columbia.edu

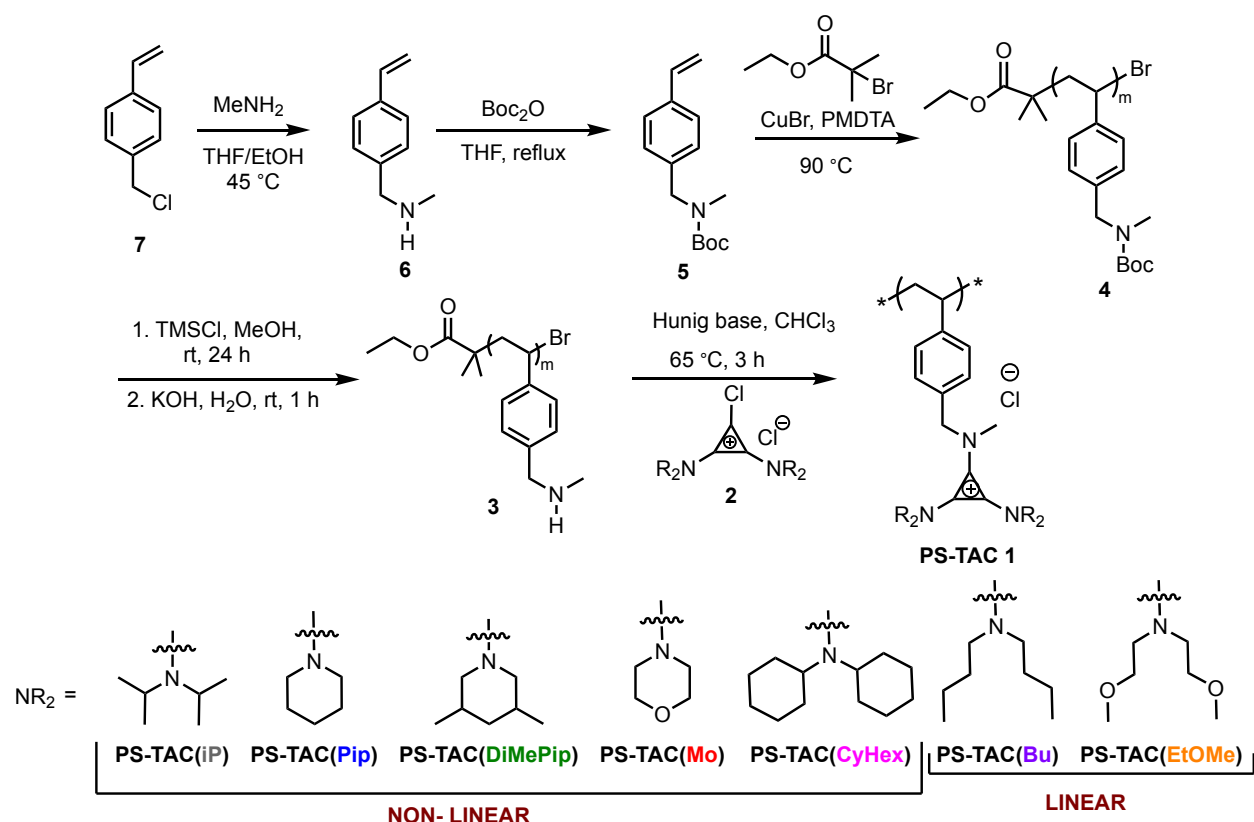


**Figure S1.** Schematic of the synthesis of the PS-TAC PILs.

The synthesis of **PS-TAC 1** family were prepared by post polymerization functionalization method, reported in the literature<sup>1-3</sup> starting from commercially available vinyl benzyl chloride **7**. Vinyl benzyl chloride on reacting with methyl amine at 45 °C result in vinyl benzyl methyl amine (**6**) followed by BOC anhydride protection yields **5**. BOC protected monomer (**5**) undergoes ATRP polymerization resulting in **4**. Followed by deprotection and reaction with functionalized cyclopropenium derivative (**2**)<sup>3</sup> results in library of **PS-TAC 1**.

<sup>1</sup>H spectra were recorded in CDCl<sub>3</sub> (except where noted in Experimental Methods) on a Bruker AMX-300, AMX-400, or AMX-500 spectrometer. Data for <sup>1</sup>H NMR are reported with chemical shift in reference to residual CHCl<sub>3</sub> at 7.26 ppm (δ ppm). The NMR spectra of the resulting polymer are listed in Figures S2-S8 below. The polymers were characterized to quantify their molecular mass (M<sub>n</sub>) and dispersity (Đ) on a Waters Alliance 2695 separation module equipped with a PL-aqua gel-OH 8-micron Mixed-M column (300 x 7.5 mm), a Waters 2998 Photodiode Array Detector, and a Waters 2414 Refractometer Detector. Tetrahydrofuran stabilized with dibutylhydroxytoluene was used as the eluent at a flow rate of 1 ml min<sup>-1</sup>. PS standards were used for the calibration. The samples were dissolved in tetrahydrofuran stabilized with BHT at 5mg/mL. The instrument was calibrated to polystyrene standards having THF as the mobile phase.

The molecular weights of the systems vary from ~30g/mol-60g/mol (degree of polymerization ~70-137), and PDI between 1.05-1.7. The features we are studying are nanometer-scale correlations in ion transport and morphology, so we do next expect this variation in PDI and molecular weight to have a significant impact on our results.

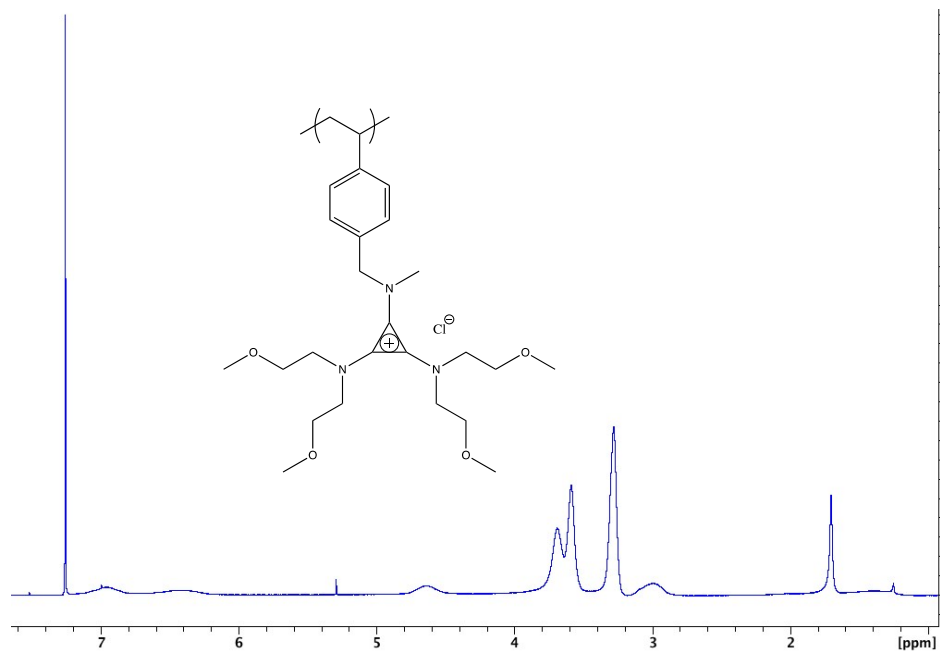


**Figure S2.**  $^1\text{H}$  NMR spectrum of PS-TAC(EtOMe).

$^1\text{H}$  NMR (400 MHz,  $\text{CDCl}_3$ )  $\delta$  7.25-6.21 (b, 62H, ArH), 4.8- 4.40 (b, 34H, ArCH<sub>2</sub>N), 3.85-3.48 (b, 242H, C<sub>3</sub>(N(CH<sub>2</sub>CH<sub>2</sub>OCH<sub>3</sub>)<sub>2</sub>)<sub>2</sub>, C<sub>3</sub>(N(CH<sub>2</sub>CH<sub>2</sub>OCH<sub>3</sub>)<sub>2</sub>)<sub>2</sub>), 3.40-2.84 (b, 204H, NCH<sub>3</sub>, C<sub>3</sub>(N(CH<sub>2</sub>CH<sub>2</sub>OCH<sub>3</sub>)<sub>2</sub>)<sub>2</sub>), 1.65-0.71 (b, 82H, ArCHCH<sub>2</sub>) Yield-66%

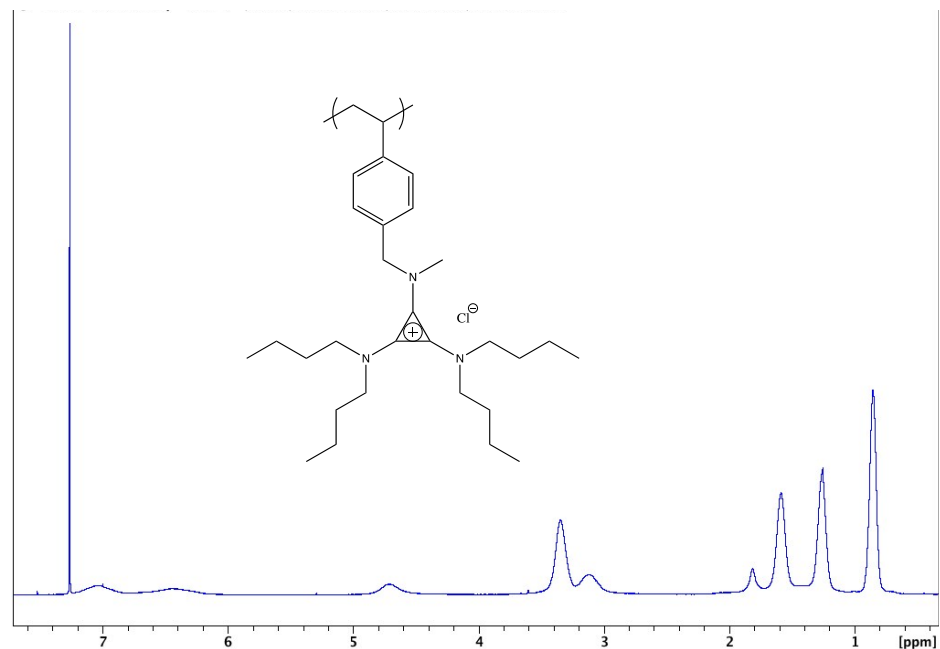


**Figure S3.**  $^1\text{H}$  NMR spectrum of PS-TAC(Bu).

$^1\text{H}$  NMR (400 MHz,  $\text{CDCl}_3$ )  $\delta$  7.25-6.12 (b, 1169H, ArH), 4.9- 4.47 (b, 518H, ArCH<sub>2</sub>N), 3.62-2.91 (b, 3008H, C<sub>3</sub>(N(CH<sub>2</sub>CH<sub>2</sub>CH<sub>2</sub>CH<sub>3</sub>)<sub>2</sub>)<sub>2</sub>, NCH<sub>3</sub>) 1.94-0.63 (b, 9265H, ArCHCH<sub>2</sub>, C<sub>3</sub>(N(CH<sub>2</sub>CH<sub>2</sub>CH<sub>2</sub>CH<sub>3</sub>)<sub>2</sub>)<sub>2</sub>, C<sub>3</sub>(N(CH<sub>2</sub>CH<sub>2</sub>CH<sub>2</sub>CH<sub>3</sub>)<sub>2</sub>)<sub>2</sub>, C<sub>3</sub>(N(CH<sub>2</sub>CH<sub>2</sub>CH<sub>2</sub>CH<sub>3</sub>)<sub>2</sub>)<sub>2</sub>) Yield-42%<sup>2</sup>

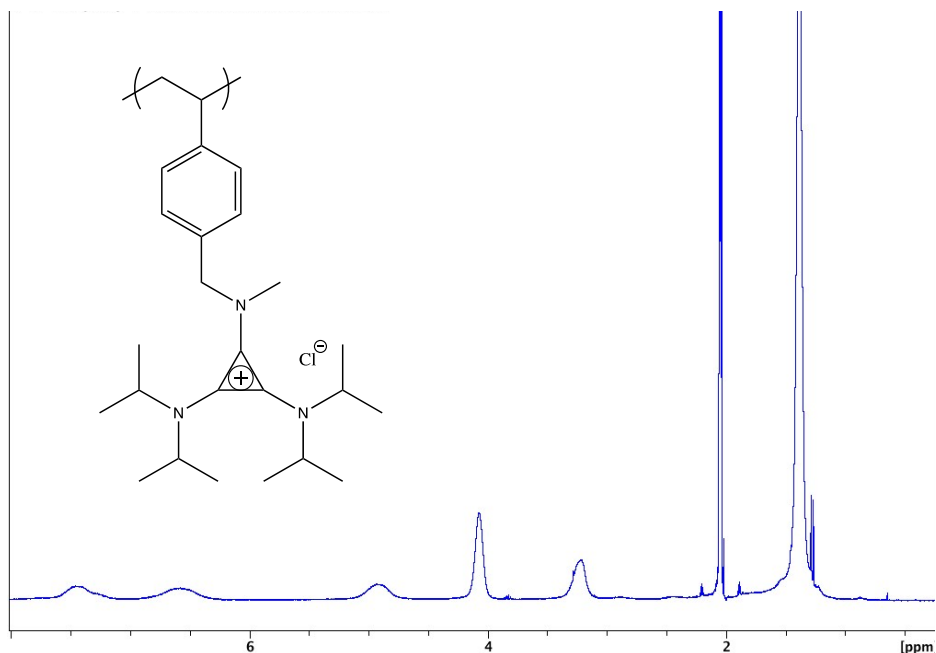


**Figure S4.** <sup>1</sup>H NMR spectrum of PS-TAC(iP).

<sup>1</sup>H NMR (400 MHz, (CD<sub>3</sub>)<sub>2</sub>CO) δ 7.60-6.35 (b, 500H, ArH), 5.22-4.62 (b, 248H, ArCH<sub>2</sub>N), 4.22-3.94 (b, 460H, C<sub>3</sub>(N(CH(CH<sub>3</sub>)<sub>2</sub>)<sub>2</sub>)), 3.39-3.07 (b, 333H, NCH<sub>3</sub>), 1.68-0.77 (b, 3052H, ArCHCH<sub>2</sub>, C<sub>3</sub>(N(CH(CH<sub>3</sub>)<sub>2</sub>)<sub>2</sub>)) Yield 65%

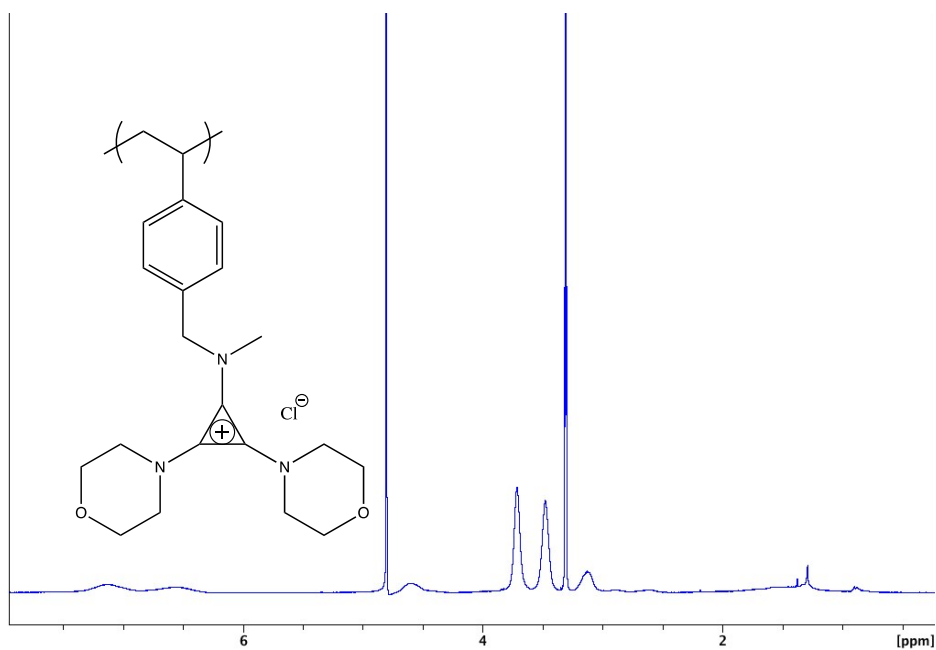


**Figure S5.** <sup>1</sup>H NMR spectrum of PS-TAC(Mo).

<sup>1</sup>H NMR (400 MHz, CD<sub>3</sub>OD) δ 7.51-6.20 (b, 440H, ArH), 4.72-4.29 (b, 162H, ArCH<sub>2</sub>N), 3.79-3.63 (b, 516H, C<sub>3</sub>(N(CH<sub>2</sub>)<sub>2</sub>(CH<sub>2</sub>)<sub>2</sub>O)<sub>2</sub>), 3.57-3.38 (b, 505H, C<sub>3</sub>(N(CH<sub>2</sub>)<sub>2</sub>(CH<sub>2</sub>)<sub>2</sub>O)<sub>2</sub>), 3.24-3.03 (b, 198H, NCH<sub>3</sub>), 1.71-0.82 (b, 370H, ArCHCH<sub>2</sub>) Yield 91%

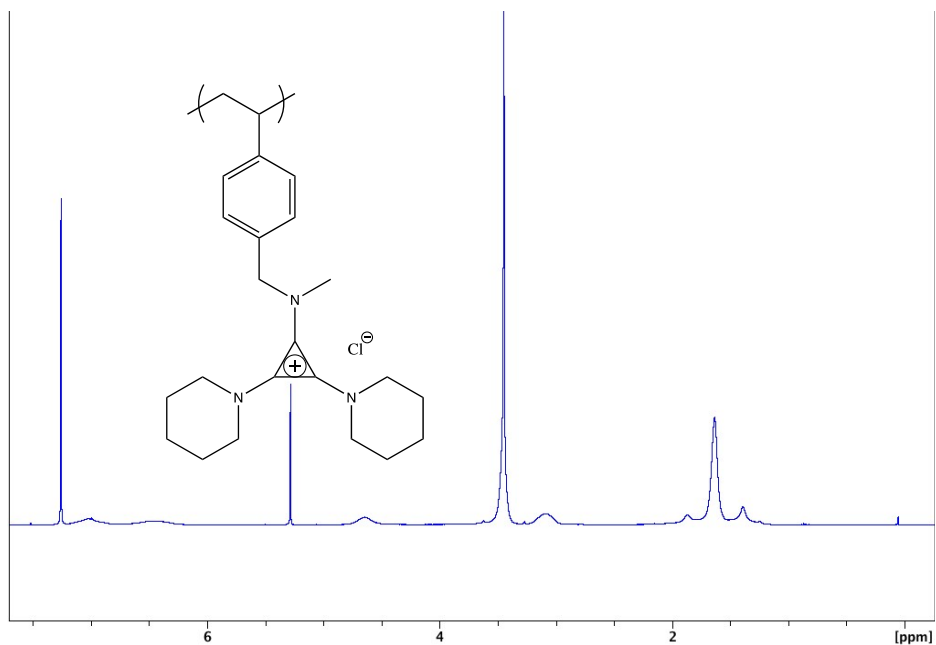


**Figure S6.**  $^1\text{H}$  NMR spectrum of PS-TAC(Pip).

$^1\text{H}$  NMR (400 MHz,  $\text{CDCl}_3$ )  $\delta$  7.51-6.20 (b, 1391H, ArH), 4.72- 4.29 (b, 642H, ArCH<sub>2</sub>N), 3.64-3.26 (b, 5409H\*, C<sub>3</sub>(N(CH<sub>2</sub>)<sub>2</sub>(CH<sub>2</sub>)<sub>2</sub>CH<sub>2</sub>)<sub>2</sub>), 3.24-2.92 (b, 960H, NCH<sub>3</sub>), 1.98-1.18 (b, 5904H, C<sub>3</sub>(N(CH<sub>2</sub>)<sub>2</sub>(CH<sub>2</sub>)<sub>2</sub>CH<sub>2</sub>)<sub>2</sub>, ArCHCH<sub>2</sub>) \*water overlap @  $\delta$  3.49 Yield 86%

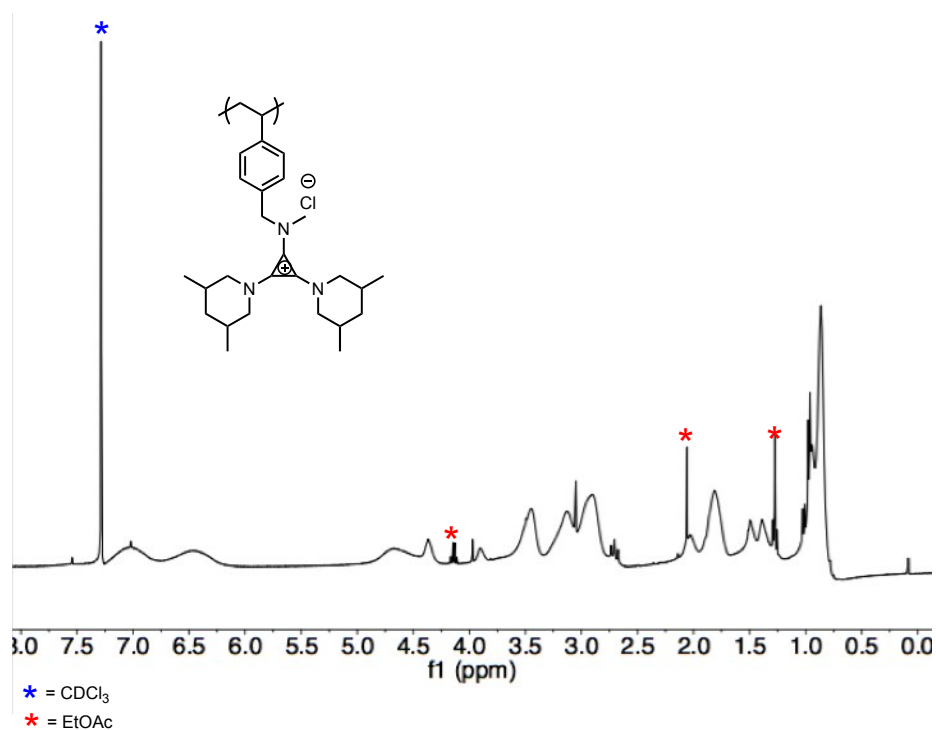
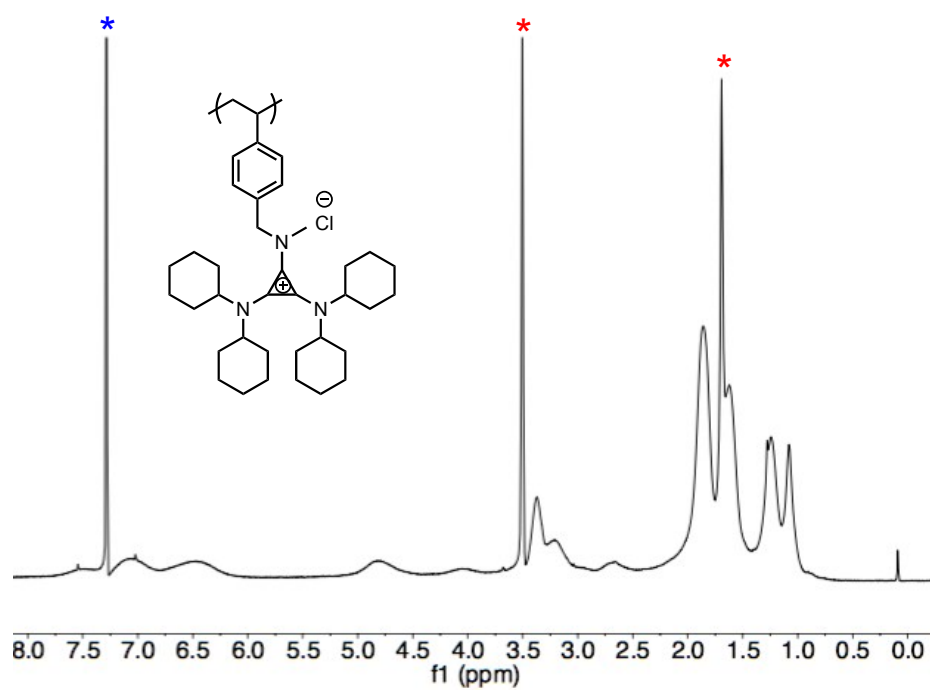


**Figure S7.**  $^1\text{H}$  NMR spectrum of PS-TAC(DiMePip).

$^1\text{H}$  NMR (400 MHz,  $\text{CDCl}_3$ )  $\delta$  7.25-6.21 (b, 84H, ArH), 4.9- 4.40 (b, 61H, ArCH<sub>2</sub>N), 3.75-2.79 (b, 221H, C<sub>3</sub>(N(CH<sub>2</sub>)<sub>2</sub>(CH<sub>2</sub>)<sub>2</sub>CH<sub>2</sub>)<sub>2</sub>, NCH<sub>3</sub>), 1.97-1.32 (b, 131H, ) C<sub>3</sub>(N(CH<sub>2</sub>)<sub>2</sub>(CH<sub>2</sub>)<sub>2</sub>CH<sub>2</sub>)<sub>2</sub>), 1.65-0.71 (b, 181H, ) ArCHCH<sub>2</sub>), C<sub>3</sub>(N(CH<sub>2</sub>)<sub>2</sub>(CH-CH<sub>3</sub>)<sub>2</sub>CH<sub>2</sub>)<sub>2</sub>) Yield 40%



\* = CDCl<sub>3</sub>  
 \* = MeOH, H<sub>2</sub>O

**Figure S8.** <sup>1</sup>H NMR spectrum of PS-TAC(CyHex).

<sup>1</sup>H NMR (400 MHz, CDCl<sub>3</sub>) δ 7.27-6.08 (b, 43H, ArH), 5.13-4.52 (b, 20H, ArCH<sub>2</sub>N), 3.49-3.02 (b, 50H, NCyH, NCH<sub>3</sub>), 2.31-0.094 (b, 348H, CyH, ArCHCH<sub>2</sub>). Yield 75%

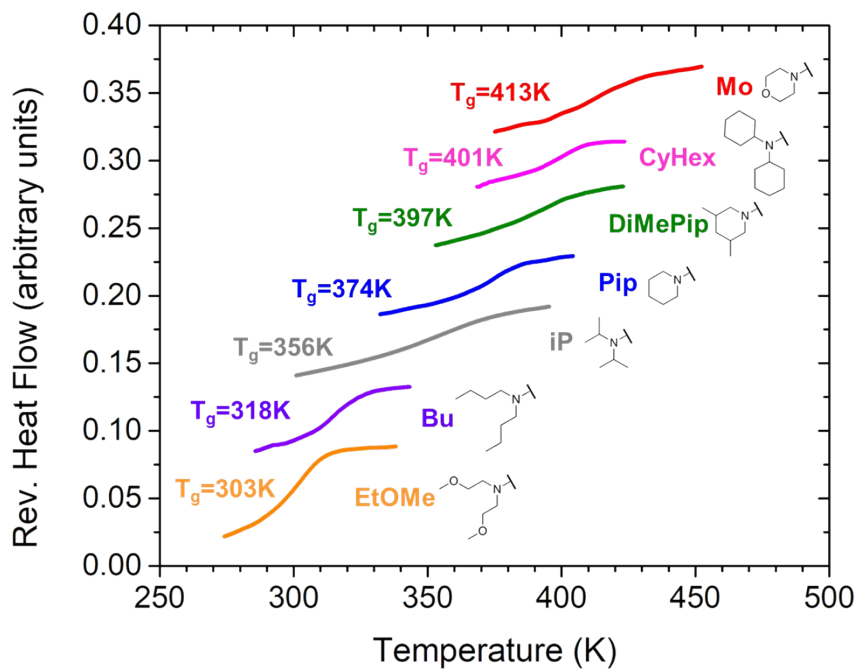


**Figure S9:** Reversible heat flow from temperature modulated DSC measurements of the PS-TAC polymers. All data shown is from the second cooling (cooling rate  $5^\circ\text{C}/\text{min}$ ) of each system. Data is shifted vertically.

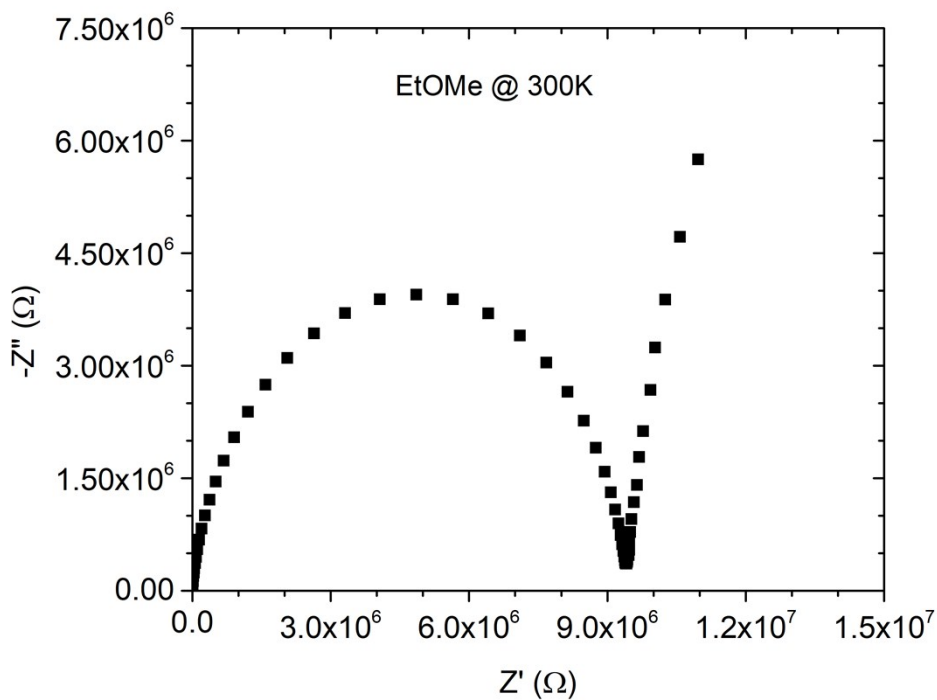


**Figure S10:** Representative example of impedance data of [PS-TAC][Cl] polymer. The high-frequency resistance is obtained from an equivalent circuit model fit.

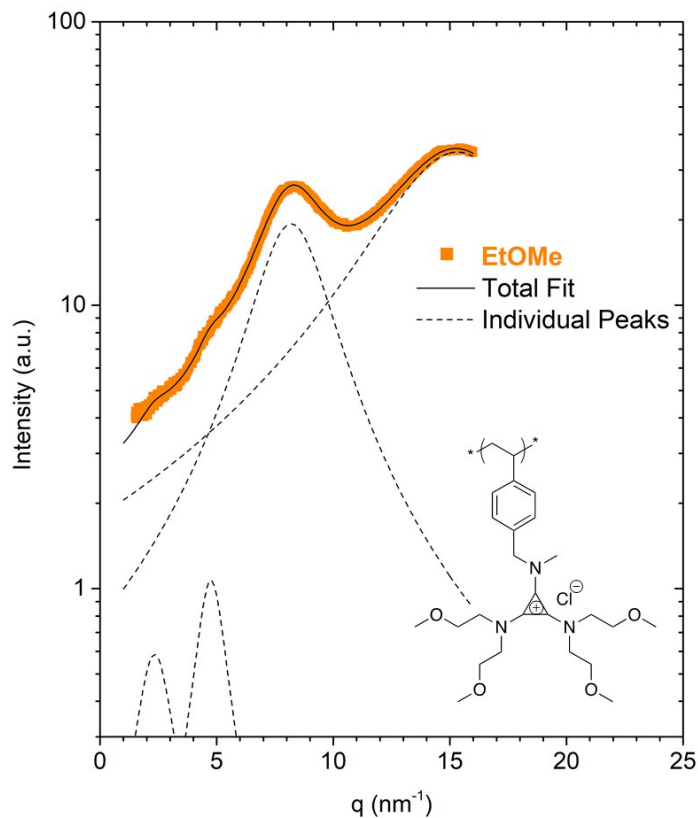


**Figure S11:** Representative example of fitting X-ray scattering data to Lorentzian peak functions. The total fit is the sum of the Lorentzian fits of the 4 individual peaks.

**Table S1:** Peak positions, and ratio of the intensity,  $I_a/I_i$ , of all of the PS-TAC PILs, determined from the Lorentzian fits.

Functional Group	$d_b$ (nm)	$d_o$ (nm)	$d_i$ (nm)	$d_a$ (nm)	Peak intensity ratio $I_a/I_i$
iP	2.04	--	0.71	0.50	3.43
Mo	2.05	--	0.72	0.45	8.75
Pip	2.48	1.13	0.75	0.46	4.22
DiMePip	2.22	1.26	0.82	0.49	7.30
CyHex	2.97	--	0.88	0.48	7.64
EtOMe	2.69	1.32	0.77	0.41	3.84
Bu	2.19	1.21	0.83	0.42	3.32



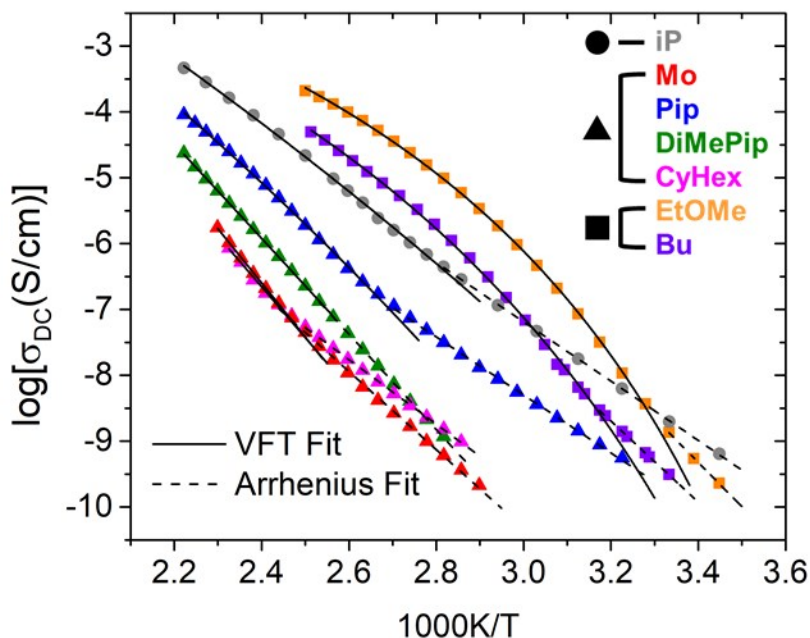


**Figure S12:** Conductivity vs. inverse temperature of the PS-TAC polymers, including VFT Fits (above  $T_g$ ) and Arrhenius fits (below  $T_g$ ). The data above the glass transition temperature of the polymer were fit to a VFT fit, and the data below the glass transition temperature of the polymer were fit to an Arrhenius fit. While the data above  $T_g$  were fit to VFT, the fit line is plotted to below  $T_g$ , to compare the Arrhenius fit at those temperatures.

**Table S2:** Activation energies of decoupled ion transport below  $T_g$  for the PS-TAC systems.

Functional Group	$E_a$ (kJ/mol)
iP	86.2
Mo	113.6
Pip	84.3
DiMePip	138.5
CyHex	93.5
EtOMe	128.6
Bu	118.8

### References:

1. Freyer, J. L.; Brucks, S. D.; Gobieski, G. S.; Russell, S. T.; Yozwiak, C. E.; Sun, M.; Chen, Z.; Jiang, Y.; Bandar, J. S.; Stockwell, B. R.; et al. Clickable Poly(Ionic Liquids): A Materials Platform for Transfection. *Angew. Chemie - Int. Ed.* **2016**, *55* (40), 12382–12386.
2. Brucks, S. D.; Freyer, J. L.; Lambert, T. H.; Campos, L. M. Influence of Substituent Chain Branching on the Transfection Efficacy of Cyclopropenium-Based Polymers. *Polymers (Basel)*. **2017**, *9* (3).
3. Jiang, Y.; Freyer, J. L.; Cotanda, P.; Brucks, S. D.; Killops, K. L.; Bandar, J. S.; Torsitano, C.; Balsara, N. P.; Lambert, T. H.; Campos, L. M. The Evolution of Cyclopropenium Ions into Functional Polyelectrolytes. *Nat. Commun.* **2015**, *6*, 1–7.